THE JOURNAL OF BIOLOGICAL CHEMISTRY
Vol. 276, No. 19, Issue of May 11, pp. 16168–16176, 2001
© 2001 by The American Society for Biochemistry and Molecular Biology, Inc.
Printed in U.S.A.

Control of Mitochondrial Redox Balance and Cellular Defense against Oxidative Damage by Mitochondrial NADP$^+$-dependent Isocitrate Dehydrogenase*

Received for publication, November 7, 2000, and in revised form, January 19, 2001
Published, JBC Papers in Press, February 13, 2001, DOI 10.1074/jbc.M010120200

Seung-Hee Jo‡§, Mi-Kyung Son‡§, Ho-Jin Koh‡, Su-Min Lee¶‖, In-Hwan Song, Yong-Ou Kim‡, Young-Sup Lee‖, Kyu-Shik Jeong‡‡, Won Bae Kim§§, Jeen-Woo Park‖, Byoung J. Song‡‡, and Tae-Lin Huhe¶‡¶¶**

*From the Departments of ‡Genetic Engineering and ‖Biochemistry, Kyungpook National University, Taegu 702-701, ¶TG Biotech Co. Ltd., Kyungpook National University, Taegu 702-701, Korea, the **Department of Anatomy, College of Medicine, Yeungnam University, Taegu 705-717, Korea, the ‡‡Laboratory of Membrane Biochemistry and Biophysics, National Institute on Alcohol Abuse and Alcoholism, Rockville, Maryland 20852, the §§Research Laboratory, Dong-A Pharmacia Co. Ltd., Youngin, Kyungi-Do 449-900, Korea*

Mitochondria are the major organelles that produce reactive oxygen species (ROS) and the main target of ROS-induced damage as observed in various pathological states including aging. Production of NADPH required for the regeneration of glutathione in the mitochondria is critical for scavenging mitochondrial ROS through glutathione reductase and peroxidase systems. We investigated the role of mitochondrial NADP$^+$-dependent isocitrate dehydrogenase (IDPm) in controlling the mitochondrial redox balance and subsequent cellular defense against oxidative damage. We demonstrate in this report that IDPm is induced by ROS and that decreased expression of IDPm markedly elevates the ROS generation, DNA fragmentation, lipid peroxidation, and concurrent mitochondrial damage with a significant reduction in ATP level. Conversely, overproduction of IDPm protein efficiently protected the cells from ROS-induced damage. The protective role of IDPm against oxidative damage may be attributed to increased levels of a reducing equivalent, NADPH, needed for regeneration of glutathione in the mitochondria. Our results strongly indicate that IDPm is a major NADPH producer in the mitochondria and thus plays a key role in cellular defense against oxidative stress-induced damage.

Cell damage induced by oxidative stress and reactive oxygen species (ROS)[1] has been implicated in several human diseases including aging, alcohol-mediated organ damage, neurodegenerative diseases, many types of cancers, cardiovascular diseases, and UV-mediated skin disorders (1). As one of the major sources of ROS (2), mitochondria are highly susceptible to oxidative damage. ROS can damage mitochondrial enzymes directly (3), and they can cause mutation in mitochondrial DNAs (4). At the same time, ROS can change the mitochondrial transmembrane potential ($\Delta\psi$m), which is indicative of mitochondrial membrane integrity (5) and precedes cell death induced by various toxic compounds and cytokines (6).

Recent reports indicate that mitochondrial ROS cause apoptosis (7, 8) by activating various apoptotic effectors such as cytochrome *c* release, procaspase-2, procaspase-9, procaspase-3, and latent apoptosis-inducing factor, which is released from the mitochondria during apoptosis (9–11). Another report also suggested that mitochondrial ROS directly caused apoptosis of T cells (12). It was also reported that tumor necrosis factor α causes a rapid production of mitochondrial ROS (13) and that ceramide, an apoptotic stimulus, also plays a crucial role in tumor necrosis factor α-induced mitochondrial ROS generation (14). Furthermore, several other investigators demonstrated that ROS are involved in the signaling pathway of certain growth factors (15) and cytokines (16). In addition, mitochondrial ROS, under hypoxic conditions, activate the transcription of the genes for glycolytic enzymes as well as erythropoietin and vascular endothelial growth factor by upregulating a transcriptional factor, hypoxia-inducible factor 1 (17), suggesting that mitochondrial ROS mediate cross-talk between the nucleus and the mitochondria. These reports suggest an important role of ROS in the regulation of cellular homeostasis including cell death and signal transduction pathway after treatments with various agents or growth factors.

During aerobic respiration to generate ATP in mitochondria, leakage of electrons frequently produces mitochondrial superoxide anions that are rapidly reduced to H_2O_2 by manganese superoxide dismutase. Because catalase, which metabolizes H_2O_2, is absent in the mitochondria of most animal cells (18), mitochondrial glutathione peroxidase plays a key role in metabolizing H_2O_2. Therefore, reduced glutathione (GSH), an efficient antioxidant and free radical scavenger by itself and required for the activity of mitochondrial glutathione peroxidase, becomes the best defense available against the potential toxicity of H_2O_2 in the mitochondria. Nevertheless, GSH is known to be synthesized in the cytosol and transported into the mitochondria (19) through rapid exchange of GSH between the

* This work was supported by Grant 991473 from the Basic Research program of the Korea Science and Engineering Foundation. The costs of publication of this article were defrayed in part by the payment of page charges. This article must therefore be hereby marked "*advertisement*" in accordance with 18 U.S.C. Section 1734 solely to indicate this fact.

The nucleotide sequence(s) reported in this paper has been submitted to the GenBank™/EBI Data Bank with accession number(s) AF212319.

§ These authors contributed equally to this work.

¶¶ To whom correspondence should be addressed: Dept. of Genetic Engineering, College of Natural Sciences, Kyungpook National University, 1370 Sankyuk-dong, Puk-ku,Taegu 702-701, Korea. Tel.: 82-53-950-5387; Fax: 82-53-943-9755; E-mail: tlhuh@knu.ac.kr.

[1] The abbreviation used are: ROS, reactive oxygen species; Glu-6-P dehydrogenase, glucose-6-phosphate dehydrogenase; ICDH, isocitrate dehydrogenase; IDH, mitochondrial NAD$^+$-dependent isocitrate dehydrogenase; IDPm, mitochondrial NADP$^+$-dependent isocitrate dehydrogenase; IDPc, cytosolic NADP$^+$-dependent isocitrate dehydrogenase; MTT, 3-(4,5-dimethylthiazol-2-yl)-2,5-diphenyltetrazolium bromide; DCF, 2′,7′-dichlorofluorescein; FACS, fluorescence-activated cell sorter; MDA, malondialdehyde.

This paper is available on line at http://www.jbc.org

cytosol and mitochondria (20). In contrast, oxidized glutathione disulfide (GSSG) in the mitochondria cannot be exported into the cytosol (21) for reconversion into GSH. These facts underscore the importance of mitochondrial NADPH as a necessary reducing equivalent for the regeneration of GSH from GSSG by the activity of mitochondrial glutathione reductase.

Until now, glucose-6-phosphate dehydrogenase (Glu-6-P dehydrogenase) was regarded as the major source of cellular NADPH because it reduces cellular oxidative stress by increasing the GSH concentration (22). Because Glu-6-P dehydrogenase is absent in the mitochondria, the mechanism for maintaining the mitochondrial NADPH pool, crucial to the control of mitochondrial redox balance, remains to be elucidated.

In mammals, three classes of isocitrate dehydrogenase (ICDH) isoenzymes exist: mitochondrial NAD^+-dependent ICDH (IDH), mitochondrial $NADP^+$-dependent ICDH (IDPm) and cytosolic $NADP^+$-dependent ICDH (IDPc) (23). Among the eukaryotic ICDH isoenzymes, IDH has been assumed to play a major role in the oxidative decarboxylation of isocitrate in the tricarboxylic acid cycle (24). However, the exact roles of IDPm and IDPc, which catalyze decarboxylation of isocitrate into α-ketoglutarate with concurrent production of NADPH in the mitochondria and cytosol, respectively, have not been elucidated.

We have reported previously the isolation and molecular characterization of cDNA clones for bovine IDPm (25) and other IDH subunits (26). In this study, we investigated the potential role of IDPm in the defense against ROS-induced oxidative damage and cell death. Our study was performed by overproducing the coding region of a cDNA for mouse IDPm followed by measurement of cell death and various indicators of oxidative stress. Reduced expression of IDPm by transfecting the antisense cDNA increased spontaneous production of ROS and lipid peroxidation accompanied by significantly more mitochondrial injury compared with the control cells transfected with vector alone. In contrast, increased expression of IDPm derived from the sense cDNA effectively prevented or reduced ROS-related damage. Our results further provide evidence that ROS-inducible IDPm is a major producer of mitochondrial NADPH, subsequently leading to an increased mitochondrial GSH pool needed for the defense against ROS-mediated oxidative injury.

EXPERIMENTAL PROCEDURES

Molecular Cloning and Construction of Cell Lines—Bovine IDPm cDNA (25) was used as a probe to screen mouse IDPm cDNA from a λ-ZAP II cDNA library of NIH3T3 cells (Stratagene). The largest IDPm cDNA was initially subcloned into the *Eco*RI site of pGEM7 (Promega). The resultant DNA was digested by *Apa*I, blunt-ended, and then digested further by either *Hin*dIII or *Cla*I before the IDPm cDNA was ligated into a LNCX-retroviral vector (27) in a sense or antisense orientation, respectively. In the LNCX-retroviral vector, expression of sense or antisense IDPm cDNA was directed by the cytomegalovirus promoter. The respective two recombinant IDPm DNA constructs or LNCX-vector alone was transfected into the BOSC23 retroviral packaging cells (28) by the calcium phosphate method. The retrovirus particles were separated from the packaging cells by filtration through a sterile filter (0.4-μm diameter) and used to transfect into NIH3T3 cells. Stable NIH3T3 transformants were identified in the presence of G418. NIH3T3 cells were grown in Dulbecco's modified Eagle's medium supplemented with 10% (v/v) fetal bovine serum (Hyclone Laboratories) and 10 μg/ml gentamycin at 37 °C in an incubator under 5% CO_2.

Antibody Preparation and Immunoblot Analysis—To prepare IDPm polyclonal antibody, a peptide representing the N-terminal 16 amino acids of mouse IDPm (ADKRIKVAKPVVEMDG) was synthesized with a peptide synthesizer (Excell, Milligene Bioresearch) and purified according to the protocol suggested by the manufacturer. The purified peptide (5 mg) was conjugated by rabbit serum albumin (1 mg) using a kit (Imject, Pierce Chemical Co.) and used to prepare polyclonal anti-peptide antibodies in rabbit. The mitochondrial homogenates from cultured cells were separated on 10% SDS-polyacrylamide gel, transferred to nitrocellulose membranes (Schleicher & Shuell), and subsequently subjected to immunoblot analysis using anti-peptide antibodies. Immunoreactive antigen was then recognized by using horseradish peroxidase-labeled anti-rabbit IgG and an enhanced chemiluminescence detection kit (Amersham Pharmacia Biotech).

Northern Blot Analysis—Total RNAs from cultured cells were prepared using RNAzol (Tel-Test Inc., Friendswood, TX) according to the manufacturer's protocol. Total RNA from cultured cells was separated by electrophoresis on 0.66 M formamide, 1% agarose gels, transferred to GeneScreen membranes, and hybridized with ^{32}P-labeled mouse IDPm cDNA as a probe. A membrane for human or mouse multiple tissue Northern blot (CLONTECH) was hybridized with ^{32}P-labeled DNA probe. Hybridization and subsequent procedures were the same as those described previously (26).

Measurement of Enzyme Activities—Mitochondrial pellets (25) prepared from cultured cells were resuspended in 1 × phosphate-buffered saline containing 0.1% Triton X-100, disrupted by sonication (4710 series, Cole-Palmer) twice at 40% of the maximum setting for 10 s, and centrifuged at 15,000 × *g* for 30 min. The supernatants were used to measure the activities of several mitochondrial enzymes. Activities of IDH and IDPm were measured by the production of NADH (26) and NADPH (29), respectively, at 340 nm at 25 °C. 1 unit of IDPm activity is defined as the amount of enzyme catalyzing the production of 1 μmol of NADPH/min. Activities for manganese superoxide dismutase, mitochondrial glutathione reductase, and mitochondrial glutathione peroxidase were determined by published methods (30, 31). Activities for Glu-6-P dehydrogenase and catalase were analyzed by the methods described (22, 32).

Measurement of Cell Viability and DNA Fragmentation—Cells (2×10^4) were grown until 80% confluence in 96-well plates, and cell viability after treatment with H_2O_2 was assessed by 3-(4,5-dimethylthiazol-2-yl)-2,5-diphenyltetrazolium bromide (MTT) assay (33). After the cells were treated for 48 h with various concentrations of H_2O_2, 50 μl of MTT (2 mg/ml, Sigma) solution was added and incubated for another 4 h at 37 °C. The MTT solution was discarded by aspiration, and the resulting formazan product converted by the viable cells was dissolved in 150 μl of dimethyl sulfoxide. The absorbance at 540 nm with a 620 nm reference was read with an enzyme-linked immunosorbent assay plate reader. Cell viability was expressed as a percentage of untreated control cells. For analyses of DNA fragmentation, cells exposed to different concentrations of H_2O_2 for 1 h were lysed in NTE buffer, pH 8.0 (100 mM NaCl, 10 mM Tris, 1 mM EDTA) containing 1% SDS and proteinase K (0.2 mg/ml). DNA extraction and purification were performed by the method described by Bernhard *et al.* (34). To analyze the degree of DNA fragmentation, 5 μg of each DNA sample was resolved on 1% agarose gel and visualized under UV illumination.

Calculation of Peroxides—Total peroxide concentrations were calculated by the rate of oxidation of ferrous (Fe^{2+}) to ferric ion (Fe^{3+}) (35). Cells (2×10^6) were either untreated or pretreated with 0.1 mM H_2O_2 for 1 h. Cell extracts were incubated with the reaction mixture (0.1 mM xylenol orange, 0.25 mM ammonium ferrous sulfate, 100 mM sorbitol, and 25 mM H_2SO_4) at 22 °C for 30 min prior to measurement of the absorbance at 560 nm. H_2O_2 (0–5 μM) was used to produce a standard curve.

Measurement of ROS—Cells (1×10^6) were grown on poly-L-lysine-coated slide glasses and untreated or treated with 1.0 mM H_2O_2 for 5 min. Intracellular ROS generation was monitored by the fluorescence produced from 2′,7′-dichlorofluorescein (DCF) after oxidation of 10 μM dichlorodihydrofluorescein diacetate (Molecular Probes, Eugene, OR) (36). Images of DCF fluorescence (excitation, 488 nm; emission, 520 nm) were acquired using a laser confocal scanning microscope (DM/R-TCS, Leica) coupled to a microscope (Leitz DM RBE). To measure the fluorescence intensity, 20 cells from each image were picked randomly, and their averages of fluorescence intensity were calculated as described (15). For FACS analyses, cells (2×10^6) were pretreated with 5 μM dichlorodihydrofluorescein diacetate and followed by exposure to 30 μM C_2-ceramide (N-acetyl-D-sphingosine, Sigma) for 15 min. Measurements of DCF fluorescence in trypsin-treated cells were made at least 10,000 events/test using a FACS Calibar flow cytometer (Becton Dickinson) with a fluorescein isothiocyanate filter. For measuring lipid peroxidation, cells (2×10^6) were either untreated or pretreated with 0.1 mM H_2O_2 for 1 h and analyzed by measuring of the concentration of malondialdehyde (MDA).

Measurement of Lipid Peroxidation—The concentration of MDA in different cells was measured by a spectrophotometric assay (37). Cells (2×10^6) were either untreated or pretreated with 0.1 mM H_2O_2 for 1 h. Then cell extracts (500 μl) were mixed with 1 ml of thiobarbituric acid-trichloroacetic acid-HCl solution (0.375% thiobarbituric acid, trichloroacetic acid in 0.25 N HCl, pH 2.0) and heated at 100 °C for 15 min. The absorbance of thiobarbituric acid-reactive substance was determined at 535 nm.

Transmission Electron Microscopy—Cells grown to 80% confluence were either untreated or pretreated with 0.1 mM H_2O_2 for 2 h, rinsed twice with phosphate-buffered saline, pH 7.3, and centrifuged at 50 × *g* for 5 min. Cell pellets were fixed immediately in 2.5% (v/v) glutaraldehyde in 0.1 M phosphate buffer for 2 h at 4 °C. Cells were postfixed in 1% osmium tetroxide for 30 min, washed with water, and then subjected to a dehydration procedure using graded ethanol series. For preparing the specimen, cells were embedded in Epon 812 (Electron Microscopy Sciences, Fort Washington, PA), and two random areas were cut and processed. The sections (60–70 nm) were cut with an ultramicrotome (Soya MT-7000), transferred to copper grids, and stained with uranyl acetate and lead citrate. At least 40 cells of each sample were examined and photographed using Hitachi H-7100 transmission electron microscope (Hitachi Co., Japan) at 75 kV.

Measurement of ATP Level—Intracellular ATP levels were determined by using luciferin-luciferase (38). Cells (5×10^6) either untreated or treated with 0.1 mM H_2O_2 for 2 h were collected by centrifugation, resuspended in 250 μl of extraction solution (10 mM KH_2PO_4, 4 mM $MgSO_4$, pH 7.4), heated at 98 °C for 4 min, and placed on ice. For ATP measurement, an aliquot of a 50-μl sample was added to 100 μl of reaction solution (50 mM $NaAsO_2$, 20 mM $MgSO_4$, pH 7.4) containing 800 μg of luciferin/luciferase (Sigma). Light emission was quantified in a Turner Designs TD 20/20 luminometer (Stratec Biomedical Systems, Germany). For all experiments, ATP standard curves were run and were linear in the range of 5–2500 nM. Concentrations of ATP stock solution were calculated from spectrophotometric absorbance at 259 nm using an extinction coefficient of 15,400.

Measurement of NADPH and GSH—NADPH values were determined by the method of Zerez *et al.* (39) and expressed as the ratio of NADPH to the total NADP pool [NADPH]/[$NADP^+$ + NADPH]. The GSH level was analyzed by producing of 5-thio-2-nitrobenzoate at 412 nm ($\epsilon = 1.36 \times 10^4\ M^{-1}\ cm^{-1}$) by the method described previously (40). Total GSH level was measured in 0.1 M potassium phosphate buffer (pH 7.0) containing 1 mM EDTA, 0.2 mg of NADPH, 30 μg of 5,5′-dithio-bis(2-nitrobenzoic acid), and 0.12 unit of glutathione reductase (Sigma). The GSSG level was measured as the same as total the GSH level after treatment with 1 μl of 2-vinylpyridine and 3 μl of triethanolamine for 1 h (41).

RESULTS

Isolation and Characterization of Mouse IDPm cDNA—To isolate cDNAs for mouse IDPm, a cDNA library of NIH3T3 cells (Stratagene) was screened with the cDNA for bovine IDPm (25) as a probe. 11 positive cDNA clones for mouse IDPm were isolated from about two million phage plaques screened. From these clones, one clone with the largest DNA insert (1.7 kilobase pairs) was purified, subcloned into plasmid pGEM7(+), and its nucleotide sequence was determined. Mouse IDPm cDNA was 1,679 base pairs long (data not shown) with an open reading frame (1,356 base pairs) for the entire protein coding region of IDPm (Fig. 1). Structural analysis of the pig (42), bovine, and mouse IDPm (25) revealed that the precursor mouse IDPm protein contains 452 amino acids (50,934 Da), and the complete protein consists of 413 amino acids (46,575 Da) with the first 39 amino acids as the mitochondrial signal peptide. The deduced protein sequence of mouse IDPm showed 94.5 and 95% identity to that of bovine and porcine IDPm, respectively. However, the mitochondrial leader sequence of the mouse IDPm was quite different from the previously reported mouse IDPm (mNADP-IDH) (43). The mNADP-IDH contained an extremely long mitochondrial leader peptide (111 amino acids), and its mature protein sequence (412 amino acids) was 1 amino acid shorter than that of our clone for mouse IDPm. In addition, 11 amino acids in its mature protein sequence are different from that of our mouse IDPm (Fig. 1).

Tissue-specific Expression of IDPm—To investigate the expression pattern of IDPm in different human and mouse tissues, Northern analyses were performed. One major IDPm transcript (2.2 kilobase pairs) was observed in both human and mouse tissues and expressed in a tissue-specific manner (Fig. 2*A*). The levels of IDPm expressed in human and mouse tissues were highest in heart, one of the most O_2-consuming tissues, whereas liver and kidney contained considerable levels of

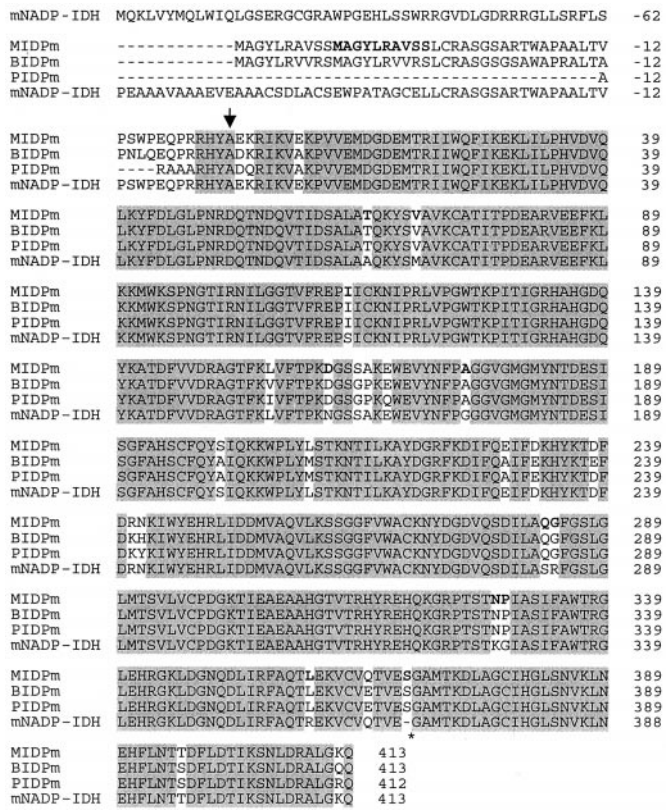

FIG. 1. **Comparison of deduced amino acid sequences for IDPm from different species.** The putative N terminus of mature IDPm protein is indicated by an *arrow*. Identical amino acid residues among four IDPm sequences are indicated by *shaded boxes*. MIDPm, BIDPm, and PIDPm represent IDPm from mouse, cow (25), and pig (42), respectively. mNADP-IDH represents the previously reported mouse IDPm (43). Amino acids that are different between mouse IDPm and mNADP-IDH are indicated by *bold letters*. An *asterisk* indicates an amino acid lacking in mNADP-IDH.

IDPm transcript but significantly less than that in heart. In contrast, other tissues including brain and lung, which are vulnerable to oxidative injury, contained very low levels of IDPm message. Interestingly, the levels of IDPm expression in human and mouse skeletal muscles were strikingly different.

Stable Transfection of IDPm Constructs—To investigate the role of IDPm directly, two different transformants for each recombinant IDPm construct were isolated after stable transfection of the sense IDPm (S1 and S2) and antisense IDPm (AS1 and AS2) or LNCX-vector alone (control) (Fig. 2*B*). Chromosomal integration of the transfected IDPm constructs was confirmed by polymerase chain reaction (data not shown). The level of IDPm transcript (2.2 kilobase pairs) in control cells was very low (Fig. 2*C*). S1 cells contained much less viral IDPm transcript (2.8 kilobase pairs) than S2 cells. Both AS1 and AS2 cells contained substantially less IDPm transcript than S1 cells (Fig. 2*C*). S1 and S2 cells exhibited 52.6 ± 5.1 and 66.7 ± 5.5 units of IDPm activities, respectively. These values are 3.5- and 4.5-fold higher, respectively, than that of control cells with the vector alone. In contrast, AS1 and AS2 cells exhibited 39 and 47% less IDPm activities, respectively, compared with that of control (Table I). To demonstrate any differences in ROS-mediated damage between cells with sense or antisense IDPm, we intentionally chose to use S1 and AS1 cells as a comparison pair because of less difference in IDPm activity in this pair than in the paired S2 and AS2 cells. Immunoblot analysis using anti-IDPm antibody further confirmed the increased expression of IDPm in S1 cells compared with the control cells and AS1 cells that contained significantly less expression of IDPm

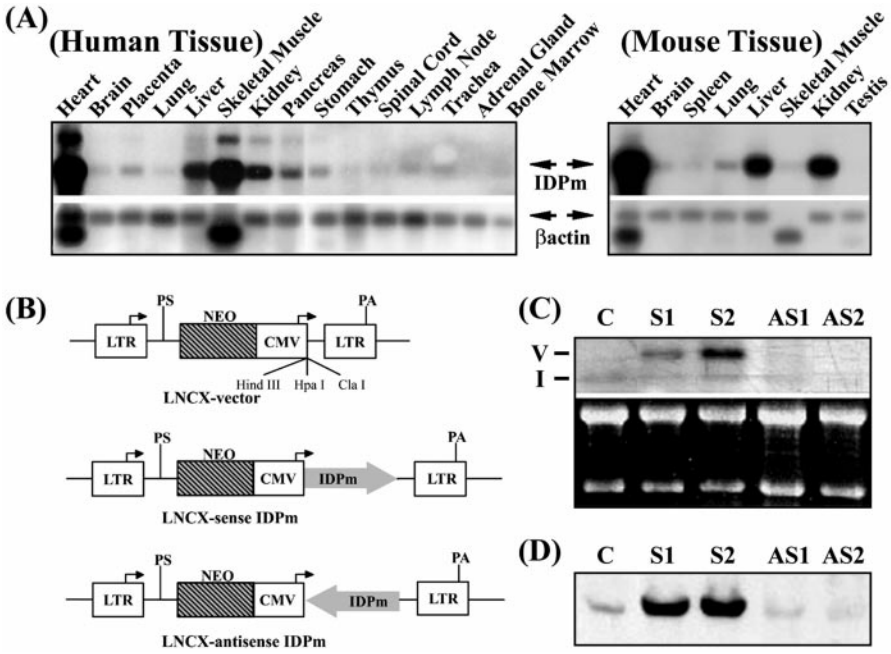

FIG. 2. **Expression of IDPm in various tissues and cultured cells.** *Panel A*, tissue-specific expression of IDPm transcript in various human and mouse tissues. A membrane for human or mouse multiple tissue Northern blot was used to study the expression of the IDPm message. Each membrane was then hybridized with ^{32}P-labeled mouse IDPm cDNA (*upper panel*) or actin cDNA (*lower panel*). *Panel B*, structures of the recombinant retroviral DNA constructs. IDPm constructs designed to express viral vector alone (LNCX) and IDPm construct in sense (LNCX-sense IDPm) or antisense (LNCX-antisense IDPm) direction under the cytomegalovirus (*CMV*) promoter are shown. *LTR*, long terminal repeat. *Panel C*, expression of IDPm in different cells with stable transfection of IDPm constructs. Total RNAs (15 μg/lane) from cells expressing LNCX-vector alone (*C*, control cells), LNCX-sense IDPm (S1 and S2 cells), and LNCX-antisense IDPm (AS1 and AS2 cells) were subjected to Northern blot analysis. *V* and *I* represent retroviral and intrinsic IDPm mRNAs, respectively. Ethidium bromide staining of a typical gel is shown at the *bottom*. *Panel D*, immunoblot analysis of IDPm protein. Mitochondrial homogenates (20 μg/lane) from different cells were separated on 10% SDS-polyacrylamide gel, transferred to nitrocellulose membrane, and then subjected to immunoblot analysis using anti-peptide polyclonal antibody.

TABLE I
Antioxidant enzyme activities in NIH3T3 transfectant cells

Values represent means ± S.D. of three independent experiments. mGPx, mitochondrial glutathione peroxidase; mGRd, mitochondrial glutathione reductase; Mn-SOD, manganese superoxide dismutase; G6PD, Glu-6-P dehydrogenase.

Cell lines	IDPm[a,b]	mGPx[a,b]	mGRd[a,c]	Mn-SOD[a,c]	IDH[a,b]	G6PD[b,d]	Catalase[c,d]
Vector	14.9 ± 1.1	41.5 ± 1.3	7.11 ± 0.4	1.50 ± 0.1	6.07 ± 1.4	45.7 ± 2.4	3.5 ± 0.2
S1 (sense IDPm)	52.6 ± 5.1 (66.7 ± 5.5)[e]	38.6 ± 0.1	7.30 ± 0.1	1.48 ± 0.1	6.16 ± 0.8	45.2 ± 1.5	3.4 ± 0.2
AS1 (antisense IDPm)	9.1 ± 1.5 (7.9 ± 0.6)[e]	39.1 ± 2.0	7.12 ± 0.1	1.50 ± 0.1	6.03 ± 0.1	44.8 ± 1.5	3.6 ± 0.3

[a] Enzyme activities measured from mitochondrial fractions.
[b] Enzyme activity represents units/g protein.
[c] Enzyme activity represents units/mg protein.
[d] Enzyme activities measured from total cell lysates.
[e] IDPm activities for S2 and AS2 cells are indicated in parentheses.

protein (Fig. 2*D*). However, immunoreactive IDPm was not detected in the cytosol of S1, AS1, or control cells (data not shown). Activities of mitochondrial IDH and other major antioxidant enzymes such as mitochondrial glutathione peroxidase, mitochondrial glutathione reductase, and manganese superoxide dismutase, were all similar in each group comparable to the control (Table I). In addition, there was less difference in Glu-6-P dehydrogenase and catalase activities in the cell lysates of S1, AS1, and control cells, suggesting that transfection of IDPm cDNAs did not affect the activities of other enzymes involved in antioxidation.

Pretranslational Induction of IDPm by ROS and Inverse Relationship between IDPm Activity and ROS-induced Damage—To study the relationship between IDPm activity and ROS-induced damage, cells were exposed to different concentrations of H_2O_2 for 48 h prior to measurement of cell viability. As shown in Fig. 3*A*, S1 cells were more resistant to H_2O_2-mediated oxidative damage than control and AS1 cells. More than 88% of S1 cells survived, whereas about 63 and 30% for control and AS1 cells survived, respectively, in the presence of 1.0 mM H_2O_2. A similar pattern of cell viability was also noticed when these cells were exposed to 25 μM menadione, a redox cycling agent, for 48 h (data not shown). In accordance with cell viability, S1 cells with increased IDPm protein became more resistant to oxidative damage with less DNA fragmentation compared with the control and AS1 cells (Fig. 3*B*). The opposite was true in AS1 cells, which, with little amounts of IDPm protein, became more sensitive to ROS treatment with more DNA fragmentation than the control and S1 cells.

To verify the protective mechanism of IDPm against cell death induced by oxidative stress, we studied the time-dependent changes in IDPm activity, protein, and its mRNA expression. For this particular study, untransfected NIH3T3 cells were exposed to 0.2 mM H_2O_2 for 1 h prior to determination of IDPm levels because treatment with 0.1 mM H_2O_2 for 1 h did not increase the IDPm level in NIH3T3 cells (data not shown). As shown in Fig. 3*C*, IDPm activity was increased in a time-dependent manner with a peak activity (2.3-fold) observed at

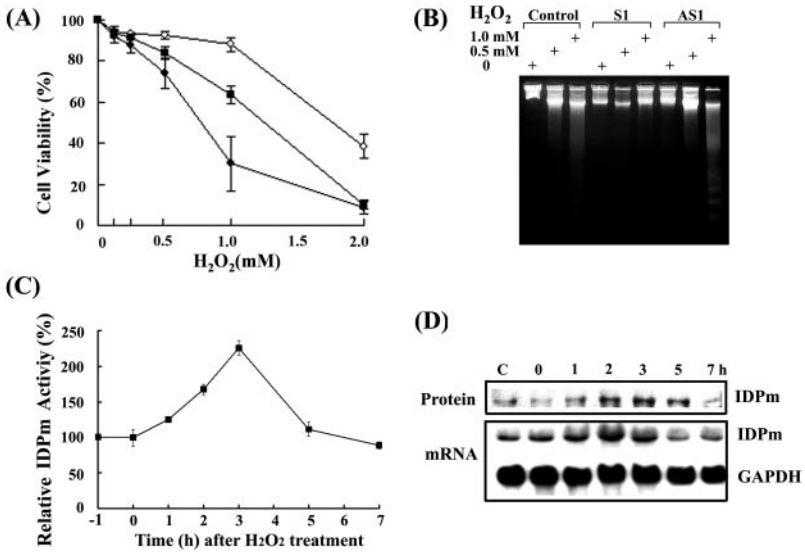

FIG. 3. **Effect of transduced IDPm on cell viability and induction of IDPm by ROS.** *Panel A*, effect of IDPm on cell viability upon H_2O_2 treatment. Three different cells (2×10^4/well) were grown in 96-well plates and then exposed to different concentrations of H_2O_2 for 48 h as indicated prior to measurement of cell viability in triplicates. S1, control, and AS cells are indicated by *open circles*, *closed rectangles*, and *closed circles*, respectively. Each value represents the mean ± S.E. from three independent experiments. *Panel B*, IDPm can protect ROS-induced DNA fragmentation. Control, S1, and AS1 cells were exposed to different concentrations of H_2O_2 for 1 h, and the degree of ROS-induced DNA fragmentation was analyzed by 1% agarose gel electrophoresis. *Panel C*, IDPm activity is induced by ROS. Untransfected NIH3T3 cells (2×10^6) were exposed to 0.2 mM H_2O_2 for 1 h and then incubated for different times as indicated in fresh medium without H_2O_2. Relative activity was calculated by comparing the IDPm activity at each time point after exposure to H_2O_2 with that of unexposed cells. Each value represents the mean ± S.D. from three separate experiments. *Panel D*, pretranslational induction of IDPm by ROS. Mitochondrial homogenates (20 μg/lane) of untransfected NIH3T3 cells at each time point before and after exposure to 0.2 mM H_2O_2 were separated on 10% SDS-polyacrylamide gel, transferred to nitrocellulose membrane, and then subjected to immunoblot analysis using anti-peptide polyclonal antibody (*upper panel*). Total RNAs (20 μg/lane) of untransfected NIH3T3 cells before and at each time point after a 1-h exposure to H_2O_2 were subjected to Northern blot analysis with using the ^{32}P-labeled probe of mouse IDPm cDNA or glyceraldehyde-3-phosphate dehydrogenase (*GAPDH*) cDNA (*lower panel*).

3 h post-treatment. The IDPm activity returned to control level at 5 h after exposure to 0.2 mM H_2O_2 (Fig. 3*C*). In contrast, IDPm activity in human acute myeloid leukemia HL60 cells was also increased in a time-dependent manner by the treatment of 0.1 mM H_2O_2 for 1 h. At 2 h post-treatment, IDPm activity reached its peak (1.9-fold increased) and returned to control level at 6 h after exposure to 0.1 mM H_2O_2 (data not shown). The increased IDPm activity in both mouse fibroblasts and human myeloid cells by H_2O_2 may imply a possible physiological role of IDPm in defense against oxidative damage. The elevation of IDPm activity in untransfected NIH3T3 cells was accompanied by corresponding increases in its protein and mRNA levels (Fig. 3*D*), suggesting a pretranslational induction mechanism, similar to the elevation of catalase under stressful conditions (44).

To investigate the role of IDPm in cellular defense against oxidative damage, we also determined the level of intracellular peroxides in different cells before and after treatment with 0.1 mM H_2O_2, where cell injury was minimal, as shown in Fig. 3*A*. In the absence of 0.1 mM H_2O_2, the peroxide level in S1 cells was decreased by 28% compared with that in control cells, whereas it was increased by 35% in AS1 cells (Fig. 4*A*). The prominent inverse relationship between the levels of transduced IDPm and intracellular peroxides was observed in the presence of 0.1 mM H_2O_2. The level of peroxide in AS1 cells was increased 2.6-fold compared with that of S1 cells in the presence of 0.1 mM H_2O_2.

The effect of IDPm on ROS production was demonstrated further by the relative intensity of DCF (36). DCF fluorescence intensity, in the absence of exogenous H_2O_2 (1 mM for a 5-min treatment), increased markedly in AS1 cells but decreased significantly in S1 cells compared with the control cells (Fig. 4*B*). Similarly, the fluorescence intensity markedly was increased in AS1 and control cells, whereas it was increased slightly in S1 cells after treatment with 1 mM H_2O_2 (Fig. 4*C*).

It has been shown that C_2-ceramide mediates tumor necrosis factor-induced ROS generation in mitochondria (14) as well as induces cytochrome *c* release from mitochondria directly (45). Therefore, we tested whether IDPm can protect intracellular ROS generation induced by C_2-ceramide. As shown in Fig. 4*D*, DCF fluorescence in AS1 cells was increased markedly after C_2-ceramide treatment, whereas S1 and control cells exhibited slight increases in DCF fluorescence. These results, taken together the data in Fig. 3, indicate that intracellular ROS production and concomitant cell death rate are inversely related to the levels of transduced IDPm protein, thus supporting a protective role of IDPm against ROS-induced cell death.

Effect of IDPm on Lipid Peroxidation—It is well established that oxidative stress in various cells usually leads to accumulation of potent, cytotoxic lipid peroxides such as MDA (46). We therefore studied the effect of IDPm on the accumulation of MDA as an indicator of lipid peroxidation. The level of MDA in AS1 cells was higher than in control or S1 cells in the absence and presence of 0.1 mM H_2O_2 (Fig. 4*E*). For instance, treatment of AS1 cells with 0.1 mM H_2O_2 increased the level of MDA 1.6-fold more than in S1 cells. However, the MDA level in S1 cells did not change even after H_2O_2 treatment. These results provide direct evidence that IDPm is involved in regulating the level of lipid peroxides caused by oxidative stress.

Protective Role of IDPm in Mitochondrial Damage Induced by Oxidative Stress—Mitochondrial damage is very important in cell death (9). Therefore we investigated further the protective role of IDPm in oxidative stress-induced mitochondrial damage. As shown in Fig. 5, in S1 and control cells, normal shapes of mitochondrial cristae were observed, whereas abnormal or substantially damaged mitochondrial cristae were evident in AS1 cells even in the absence of exogenous H_2O_2. More prominent changes in mitochondrial morphologies were observed in the cells treated with 0.1 mM H_2O_2. In S1 cells, mitochondria contained normal cristae, despite a slightly swol-

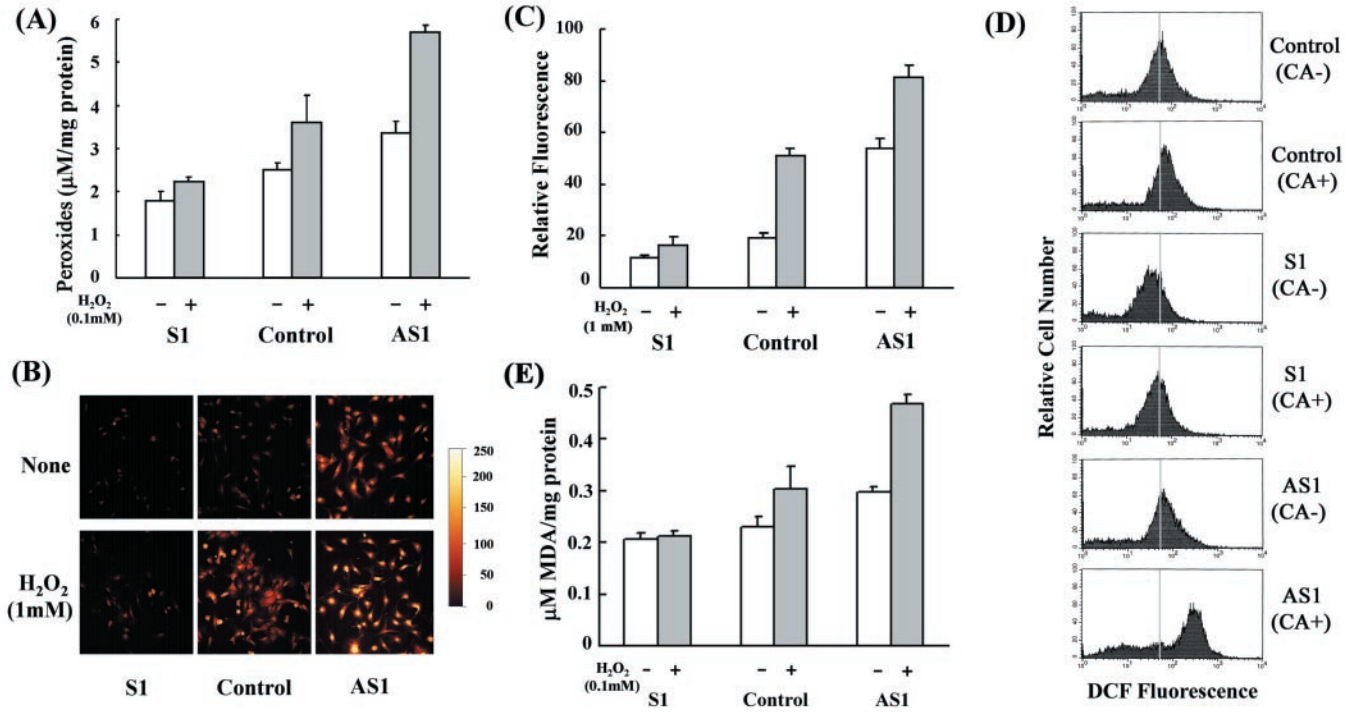

FIG. 4. **Effects of IDPm on peroxide level and ROS generation.** *Panel A*, effect of IDPm on cellular peroxide generation. Production of total peroxides in S1, control, and AS1 cells was determined by the method described under "Experimental Procedures." *Open* and *shaded bars* represent the levels of total peroxides produced in the transfected cells untreated and treated with 0.1 mM H_2O_2 for 1 h, respectively. *Panel B*, DCF fluorescence in transfected cells. Typical patterns of DCF fluorescence are presented for transfected cells untreated or treated with 1 mM H_2O_2 for 5 min. Fluorescent images were obtained under laser confocal microscopy from three separate experiments. *Panel C*, relative intensity of DCF fluorescence in transfected cells. *Open* and *shaded bars* represent the relative intensity of DCF fluorescence produced in the cells untreated and treated with 1 mM H_2O_2 for 5 min, respectively. Each value represents the mean ± S.D. 20 cells from each image were picked randomly, and the averages of their fluorescence intensity were calculated as described under "Experimental Procedures." *Panel D*, effect of IDPm on C_2 -ceramide-induced ROS production. Cells were treated with 30 μM C_2-ceramide for 15 min and subjected to FACS analyses. *CA−* and *CA+* denote the absence and presence of C_2 -ceramide treatment, respectively. *Panel E*, the levels of MDA in transfected cells were determined in triplicates. *Open* and *shaded bars* represent the level of MDA accumulated in the cells untreated or treated with 0.1 mM H_2O_2, respectively. Each value represents the mean ± S.D. from three separate experiments.

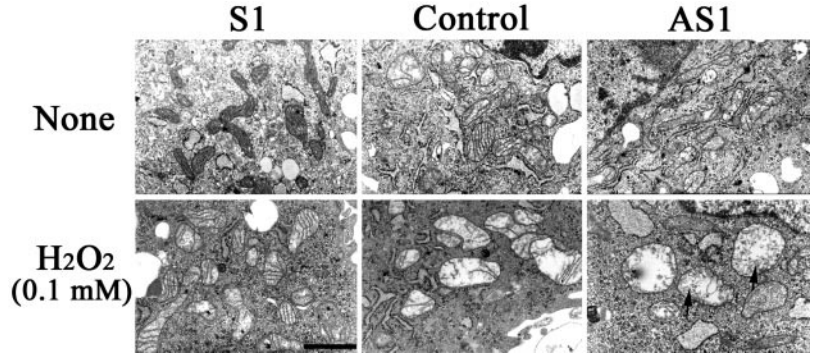

FIG. 5. **Effect of transduced IDPm on mitochondrial ultrastructure.** Cells transfected with different DNA vectors were untreated or treated with 0.1 mM H_2O_2 for 2 h, and their mitochondrial structures were then examined under transmission electron microscopy. *Arrows* in AS1 cells indicate dirty debris or remnants of cristae. The *scale bar* represents 1 μm.

len and pale matrix. In contrast, abnormal mitochondrial shapes were noticed in control and AS1 cells. In control cells, small remnants of cristae with considerable swelling were evident. Mitochondria of AS1 cells were extremely swollen and frequently lacked typical cristae but contained vesicular remnants and severely collapsed membranes. These results suggest that reduced expression of IDPm most likely leads to increased mitochondrial injury, whereas elevated IDPm protects mitochondria from oxidative damage.

Effect of IDPm on Intracellular ATP Level—Mitochondrial injury is often followed by the depletion of intracellular ATP level. As shown in Fig. 6, AS1 cells contained ~30% less ATP level than those of S1 and control cells without H_2O_2 treatment. The reduction in the ATP level after 0.1 mM H_2O_2 treatment was more prominent than in the absence of H_2O_2 treatment; for instance, the ATP level was decreased only by 13% in S1 cells, whereas it was reduced by 78 and 61% in AS1 and control cells, respectively, after H_2O_2 treatment, suggesting a protective role of IDPm against the loss of intracellular ATP levels. These data in Figs. 5 and 6 are consistent with the role of IDPm in preventing the loss of mitochondrial membrane integrity (5), which was measured by the uptake of rhodamine 123 in this laboratory (data not shown).

Role of IDPm in Regulating Mitochondrial Redox Balance for GSH Recycling—To investigate a potential mechanism by which IDPm protects cells from oxidative injury, we measured the cellular levels of NADPH and GSH. In S1 cells, the ratio for mitochondrial [NADPH]/[$NADP^+$ + NADPH] was 0.98 ± 0.06, whereas that of control cells and AS1 cells was 0.71 ± 0.08 and 0.51 ± 0.09, respectively (Fig. 7*A*). In other words, more NADPH is present in the mitochondria of S1 cells than in control and AS1 cells. However, the ratio for the cytosolic

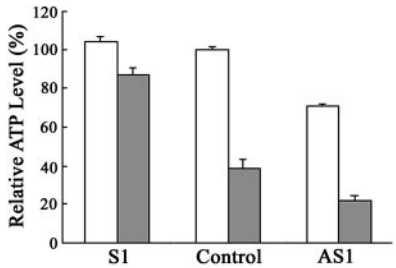

FIG. 6. **Effect of IDPm on the levels of intracellular ATP.** Different cells as indicated were untreated or treated with 0.1 mM H_2O_2 for 2 h and assayed for intracellular ATP content. Values are expressed as a percentage of ATP content in control cells (0.78 ± 0.01 nmol of ATP/10^6 cells) in the absence of H_2O_2 treatment. *Open* and *shaded bars* indicate the content of ATP in the cells untreated and treated with H_2O_2, respectively. Each value represents the mean ± S.D. from three separate experiments.

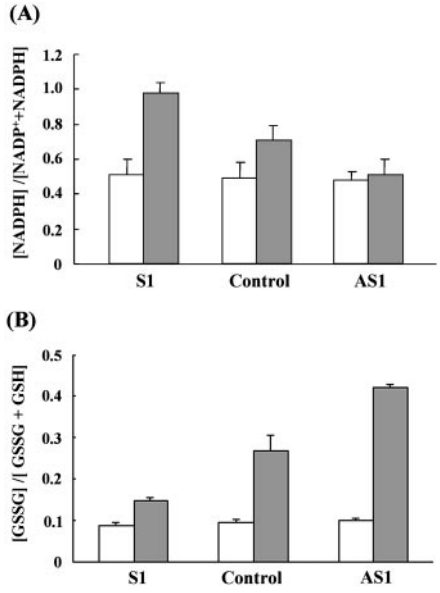

FIG. 7. **Effect of transduced IDPm on the levels of mitochondrial NADPH and GSH.** *Panel A*, ratios of NADPH *versus* total NADP pool. *Open* and *shaded bars* represent the NADPH ratios in the cytosol and mitochondria of transfected cells, respectively. *Panel B*, ratios of GSSG *versus* total GSH pool. *Open* and *shaded bars* represent the GSSG ratios in the cytosol and mitochondria of transfected cells, respectively. Each value represents the mean ± S.D. from three independent experiments.

[NADPH]/[$NADP^+$ + NADPH] in all three cells was between 0.52 ± 0.08 and 0. 49 ± 0.06. These data show that transfected IDPm in S1 and transfected antisense IDPm in AS1 cells did not alter the cytosolic NADPH level and that IDPm is, therefore, the major factor that influences the production of mitochondrial NADPH.

In mitochondria, removal of H_2O_2 is catalyzed primarily by mitochondrial glutathione peroxidase at the expense of the reduced GSH, producing the oxidized glutathione, GSSG. Therefore NADPH, required for GSH regeneration by mitochondrial glutathione peroxidase, is a critical factor for the mitochondrial defense against oxidative damage. The ratio for mitochondrial [GSSG]/[GSSG + GSH] in S1 cells was 0.148 ± 0.009, whereas that of control and AS1 cells was 0.270 ± 0.035 and 0.420 ± 0.007, respectively (Fig. 7*B*). These data establish that more reduced GSH exists in the mitochondria of S1 cells than in control and AS1 cells. However, the cytoplasmic ratio of [GSSG]/[GSH + GSSG] in S1, control, and AS1 cells was almost comparable. These results confirm that increased IDPm activity only contributes to enhancement of the mitochondrial production of a reducing equivalent, NADPH, which, in turn, increases the level of mitochondrial GSH.

DISCUSSION

The presence of a distinct gene for IDPm has been demonstrated by the biochemical characterization, chromosomal location, and molecular cloning and sequence analyses of IDPm genes in different species (26**,** 47–49). Deduced IDPm proteins in various species including human IDPm (GenBank accession number X69433)[2] share highly conserved sequences. The function of IDPm has been proposed either to catalyze the decarboxylation of isocitrate into α-ketoglutarate in the tricarboxylic acid cycle or to mediate the reversal reaction for the production of isocitrate from glutamic acid needed for gluconeogenesis (50). However, these hypotheses could not be proven because yeast NAD^+-dependent IDH is a key enzyme in the tricarboxylic acid cycle, and IDPm could not replace the functional role of IDH (51). In addition, the level of IDPm expressed in the liver is so low that it may not be involved in hepatic gluconeogenesis. Therefore, the biological role of IDPm has been unclear. The results presented in this report provide direct evidence that IDPm is a key enzyme in cellular defense against oxidative damage by supplying NADPH in the mitochondria, needed for the regeneration of mitochondrial GSH or thioredoxin. Elevation of mitochondrial NADPH and GSH by IDPm in turn suppressed the oxidative stress and concomitant ROS-mediated damage.

It is well established that mitochondrial dysfunction is directly and indirectly involved in a variety of pathological states caused by genetic mutations as well as exogenous compounds or agents. Potential benefits of IDPm and subsequent elevation of mitochondrial NADPH and GSH against oxidative damage could be explained by the following facts. First, catalase, a major enzyme for breakdown of H_2O_2, is absent in the mitochondria of mammalian cells (18). Second, mitochondrial GSH becomes critically important against ROS-mediated damage because it not only functions as a potent antioxidant but is also required for the activities of mitochondrial glutathione peroxidase and mitochondrial phospholipid hydroperoxide glutathione peroxidase (52), which removes mitochondrial peroxides. Third, depletion of mitochondrial, but not cytosolic, GSH potentiated the oxidative cell death after treatment with *tert*-butyl hydroperoxide (53). Fourth, GSH, not synthesized in mitochondria, must be synthesized in the cytosol and transported into mitochondria by a specific transporter (19, 54). Fifth, the oxidized GSSG is not retransported into the cytosol for its reduction to GSH (21). Sixth, NADPH is a major source of reducing equivalents and cofactor for mitochondrial thioredoxin peroxidase family/peroxiredoxin family including peroxiredoxin III/protein SP-22 (55–57) and peroxiredoxin V/AOEB166 (58). Finally, NADPH can prevent the formation of tocopheroxyl radical derived from the oxidation of vitamin E at mitochondrial membranes (59). All of these facts underscore a key role of mitochondrial GSH against ROS-induced injury and suggest a possible mechanism to regenerate GSH from GSSG by supplying NADPH within the mitochondria, independent from the cytosolic NADPH producer (22). Therefore, any mitochondrial NADPH producer, if present, becomes critically important for cellular defense against ROS-mediated damage.

In this study, we investigated the potential role of IDPm in cellular defense, based on reasons stated above and our previous results that the *Escherichia coli* mutant lacking $NADP^+$-specific ICDH is very sensitive to radiation-induced oxidative

[2] S.-H. Jo, M.-K. Son, H.-J. Koh, S.-M. Lee, I.-H. Song, Y.-O. Kim, Y. S. Lee, K.-S. Jeong, W. B. Kim, J.-W. Park, B. J. Song, and T.-L. Huh, unpublished data.

damage (60). To achieve our goal, we prepared cells with stable transfection of IDPm constructs in the sense (S1 cells) or antisense (AS1 cells) direction. Under our experimental conditions without apparent changes in the activities of other enzymes involved in antioxidation, cell viability showed a wide variation, depending on the levels of transduced IDPm. A clear inverse relationship was observed between the amount of IDPm expressed in target cells and their cell death rate, DNA fragmentation, the levels of intracellular ROS generation induced by H_2O_2 and C_2-ceramide, lipid peroxidation, and mitochondrial damage with loss of intracellular ATP levels. In addition, the protective role of IDPm against oxidative injury was directly supported by the pretranslational induction of IDPm under a high concentration of ROS and the relative levels of mitochondrial NADPH and GSH in three different IDPm transfectant cells. Furthermore, our data suggest that cytosolic NADPH does not play a role because of the little change in its level in the three different cells. Higher levels of mitochondrial NADPH and GSH in S1 cells conferred greater resistance to oxidative injury than in control or AS1 cells, supporting the inverse relationship between the levels of mitochondrial NADPH, GSH, and the rate of cell death. These results not only establish a protective role of IDPm in ROS-mediated oxidative damage but also address the unresolved question about the major source of the mitochondrial NADPH needed for GSH regeneration.

Northern analysis revealed that IDPm transcript is expressed in a tissue-specific manner. In contrast to heart tissue, brain contains very little IDPm transcript, consistent with the earlier reports that IDPm activity is very low in the brain tissues (43, 61). The tissue-specific expression and different IDPm activities may explain why each tissue such as brain and heart may have a different susceptibility to oxidative organ damage. The following factors, which may be related to IDPm expression, may also contribute to the differential susceptibility of each tissue to ROS-mediated damage. First, GSH in rat brain mitochondria is oxidized more easily than in liver (62). Second, brain is one of the most vulnerable organs to oxidative stress and ischemic injury (63). Third, NADPH is produced at different rates in certain tissues, indicating a possibility of differential protection or injury in a tissue-specific manner (64, 65). Therefore, our results of tissue-specific expression of IDPm transcript suggest that certain tissues with higher levels of IDPm may be more resistant to oxidative damage than those tissues with lower level of IDPm expressed. However, our results raise an important question about a major protective mechanism against ROS-mediated damage in brain and lung, although IDPm along with malic enzyme and nicotinamide nucleotide transhydrogease has recently been reported to contribute to the regeneration of mitochondrial NADPH required for the reduction of GSH in rat forebrain mitochondria (66). Thus, this question remains to be answered.

It is known that some of the key enzymes involved in antioxidant defense are elevated under stressful conditions in a compensatory manner. These enzymes include catalase, manganese superoxide dismutase, and glutathione peroxidase (44). These genes are elevated through activation of a transcription factor, nuclear factor-κB, activated upon exposure to ROS (67). The results shown in this study clearly establish that levels of IDPm activity, protein, and mRNA transcript are elevated under stressful conditions, possibly in a compensatory mechanism against elevated ROS. Although we do not know the mechanism of the pretranslational activation of the IDPm gene because of a lack of knowledge on its 5′-promoter region, it is tempting to speculate that the IDPm gene may also be activated through the activation of nuclear factor-κB. Alternatively, the 5′-promoter region of the IDPm gene may contain the so-called "antioxidative responsive element" sequence, which is also responsive to exogenous stressors (68).

Our results, taken together, indicate that IDPm is a major component in regulating mitochondrial redox balance by providing the NADPH. Furthermore, we, for the first time, demonstrated that IDPm-mediated NADPH production is critically important for cellular defense against oxidative stress-induced cell death by increasing the mitochondrial GSH concentration. In this regard, potential roles of IDPm could be expanded to the therapeutic application for various ROS-mediated cellular homeostasis and diseases including ischemic injuries and aging process possibly through blockade of ROS production and prevention of ROS-mediated specific mutations on the main control region for replication of the mitochondrial genome (69), respectively.

Acknowledgments—We are grateful to Dr. M. J. Park for electron microscopy; and Dr. R. L. Veech (National Institutes of Health), Dr. R. F. Colman (University of Delaware), and Dr. J. P. Hardwick (Northeastern Ohio Medical School) for critical reading of the manuscript.

REFERENCES

1. Ames, B. N., Shigenaga, M. K., and Hagen, T. M. (1993) *Proc. Natl. Acad. Sci. U. S. A.* **90,** 7913–7922
2. Chance, B., Sies, H., and Boveris, A. (1979) *Physiol. Rev.* **59,** 527–605
3. Lenaz, G. (1998) *Biochim. Biophys. Acta* **1366,** 53–67
4. Esposito, L. A., Melov, S., Panov, A., Cottrell, B. A., and Wallace, D. C. (1999) *Proc. Natl. Acad. Sci. U. S. A.* **96,** 4820–4825
5. Huang, P., Feng, L., Oldham, E. A., Keating, M. J., and Plunkett, W. (2000) *Nature* **407,** 390–395
6. Lemasters, J. J., Nieminen, A. L., Qian, T., Trost, L. C., Elmore, S. P., Nishimura, Y., Crowe, R. A., Cascio, W. E., Bradham, C. A., Brenner, D. A., and Herman, B. (1998) *Biochim. Biophys. Acta* **1366,** 177–196
7. Hockenbery, D. M., Oltvai, Z. N., Yin, X.-M., Milliman, C. L., and Korsmeyer, S. J. (1993) *Cell* **75,** 241–251
8. Nomura, K., Imai, H., Koumura, T., Arai, M., and Nakagawa, Y. (1999) *J. Biol. Chem.* **274,** 29294–29302
9. Green, D. R., and Reed, J. C. (1998) *Science* **281,** 1309–1312
10. Susin, S. A., Lorenzo, H. K., Zamzami, N., Marzo, I., Brenner, C., Larochette, N., Prevost, M. C., Alzari, P. M., and Kroemer, G. (1999) *J. Exp. Med.* **189,** 381–394
11. Susin, S. A., Lorenzo, H. K., Zamzami, N., Marzo, I., Snow, B. E., Brothers, G. M., Mangion, J., Jacotot, E., Costantini, P., Loeffler, M., Larochette, N., Goodlett, D. R., Aebersold, R., Siderovski, D. P., Penninger, J. M., and Kroemer, G. (1999) *Nature* **397,** 441–446
12. Hildeman, D. A., Mitchell, T., Teague, T. K., Henson, P., Day, B. J., Kappler, J., and Marrack, P. C. (1999) *Immunity* **10,** 735–744
13. Goossens, V., Grooten, J., De Vos, K., and Fiers, W. (1995) *Proc. Natl. Acad. Sci. U. S. A.* **92,** 8115–8119
14. Garcia-Ruiz, C., Colell, A., Mari, M., Morales, A., and Fernandez-Checa, J. C. (1997) *J. Biol. Chem.* **272,** 11369–11377
15. Sundaresan, M., Yu, Z.-X., Ferrans, C. J., Irani, K., and Finkel, T. (1995) *Science* **270,** 296–299
16. Lo, Y. Y. C., and Cruz, T. F. (1995) *J. Biol. Chem.* **270,** 11727–11730
17. Semenza, G. L. (1999) *Cell* **98,** 281–284
18. Esworthy, R, S., Ho, Y. S., and Chu, F. F. (1997) *Arch. Biochem. Biophys.* **340,** 59–63
19. Griffith, O. W., and Meister, A. (1985) *Proc. Natl. Acad. Sci. U. S. A.* **82,** 4668–4672
20. Martensson, J., Lai, J. C. K., and Meister, A. (1990) *Proc. Natl. Acad. Sci. U. S. A.* **87,** 7185–7189
21. Olafsdottier, K., and Reed, D. J. (1988) *Biochim. Biophys. Acta* **964,** 377–382
22. Salvemini, F., Franze, A., Iervolino, A., Filosa, S., Salzano, S., and Ursini, M. V. (1999) *J. Biol. Chem.* **274,** 2750–2757
23. Plaut, G. W. E., and Gabriel, J. L. (1983) *Biochemistry of Metabolic Process*, pp. 285–301, Elsevier Science Publishing Co., Inc., New York
24. Cupp, J. R., and McAlister-Henn, L. (1991) *J. Biol. Chem.* **266,** 22199–22205
25. Huh, T.-L., Ryu, J. H., Huh, J. W., Sung, H. C., Oh, I.-U., Song, B. J., and Veech, R. L. (1993) *Biochem. J.* **292,** 705–710
26. Kim, Y.-O., Koh, H.-J., Kim, S.-H., Jo, S.-H., Huh, J.-W., Jeong, K.-S., Lee, J. I., Song, B. J., and Huh, T.-L. (1999) *J. Biol. Chem.* **274,** 36866–36875
27. Miller, A. D., and Rosman, G. T. (1989) *BioTechniques* **7,** 980–990
28. Pear, W. S., Nolan, G. P., Scott, M. L., and Baltimore, D. (1993) *Proc. Natl. Acad. Sci. U. S. A.* **90,** 8392–8396
29. Loverde, A. W., and Lehrer, G. M. (1973) *J. Neurochem.* **20,** 441–448
30. Marklund, S. L., and Marklund, G. (1974) *Eur. J. Biochem.* **47,** 469–474
31. Pinto, R. E., and Bartley, W. (1969) *Biochem. J.* **112,** 109–115
32. Aebi, H. (1984) *Method. Enzymol.* **105,** 121–126
33. Matteo, M. A., Loweth, A. C., Thomas, S., and Mabley, J. G. (1997) *Apoptosis* **2,** 164–177
34. Bernhard, C. T., Klas, C., Peters, A. M. J., Matzku, S., Moller, P., Falk, W., Debatin, K.-M., and Krammer, P. H. (1989) *Science* **245,** 301–304
35. Jiang, Z. Y., Hunt, J. V., and Wolff, S. P. (1992) *Anal. Biochem.* **202,** 384–389
36. Bass, D. A., Parce, J. W., Dechatelet, L. R., Szejda, P., Seeds, M. C., and Thomas, M. (1983) *J. Immunol.* **130,** 1910–1917

37. Buege, J. A., and Aust, S. D. (1978) *Methods Enzymol.* **52,** 302–310
38. Spragg, R. G., Hinshaw, D. B., Hyslop, P. A., Schraufstätter, I. U., and Cochrane, C. G. (1985) *J. Clin. Invest.* **76,** 1471–1476
39. Zerez, C. R., Lee, S. J., and Tanaka, K. R. (1987) *Anal. Biochem.* **1964,** 367–373
40. Akerboom, T. P. M., and Sies, H. (1981) *Methods Enzymol.* **77,** 373–382
41. Anderson, M. E. (1985) *Methods Enzymol.* **113,** 548–555
42. Haselbeck, R. J., Colman, R. F., and McAlister-Henn, L. (1992) *Biochemistry* **31,** 6219–6223
43. Yang, L., Luo, H., Vinay, P., and Wu, J. (1996) *J. Cell. Biochem.* **60,** 400–410
44. Shull, S., Heintz, N. H., Periasamy, M., Manohar, M., Janssen, Y. M., Marsh, J. P., and Mossman, B. T. (1991) *J. Biol. Chem.* **266,** 24398–24403
45. Cuvillier, O., Edsall, L., and Spiegel, S. (2000) *J. Biol. Chem.* **275,** 15691–15700
46. Esterbauer, H., Schaur, R. J., and Zollner, H. (1991) *Free Radic. Biol. Med.* **11,** 81–128
47. Oh, I.-L., Inazawa, J., Kim, Y.-O., Song, B. J., and Huh, T.-L. (1996) *Genomics* **38,** 104–106
48. Huh, T.-L., Kim, Y.-O., Oh, I.-U., Song, B. J., and Inazawa, J. (1996) *Genomics* **32,** 295–296
49. Kim, Y.-O., Park, S.-H., Kang, Y.-J., Koh, H.-J., Kim, S.-H., Park, S.-Y., Sohn, U., and Huh, T.-L. (1999) *Cytogenet. Cell Genet.* **86,** 240–241
50. Des Rosiers, C., Di Donato, L., Comte, B., Laplante, A., Marcoux, C., David, F., Fernandez, C. A., and Brunengraber, H. (1995) *J. Biol. Chem.* **270,** 10027–10036
51. Haselbeck, R. J., and McAlister-Henn, L. (1993) *J. Biol. Chem.* **268,** 12116–12122
52. Arai, M., Imai, H., Koumura, T., Yoshida, M., Emoto, K., Umeda, M., Chiba, N., and Nakagawa, Y. (1999) *J. Biol. Chem.* **274,** 4924–4933
53. Shan, X., Jones, D. P., Hashmi, M., and Anders, M. W. (1993) *Chem. Res. Toxicol.* **6,** 75–81
54. Garcia-Ruiz, C., Morales, A., Colell, A., Rodes, J., Yi, J. R., Kaplowitz, N., and Fernandez-Checa, J. C. (1995) *J. Biol. Chem.* **270,** 15946–15949
55. Araki, M., Nanri, H., Ejima, K., Murasato, Y., Fujiwara, T., Nakashima, Y., and Ikeda, M. (1999) *J. Biol. Chem.* **274,** 2271–2278
56. Kang, S. W., Chae, H. Z., Seo, M. S., Kim, K., Baines, I. C., and Rhee, S. (1998) *J. Biol. Chem.* **273,** 6297–6302
57. Watabe, S., Hasegawa, H., Takimoto, K., Yamamoto, Y., and Takahashi, S. Y. (1995) *Biochem. Biophys. Res. Commun.* **213,** 1010–1016
58. Knoops, B., Clippe, A., Bogard, C., Arsalane, K., Wattiez, R., Hermans, C., Duconseille, E., Falmagne, P., and Bernard, A. (1999) *J. Biol. Chem.* **274,** 30451–30458
59. Packer, L., Maguire, J. J., Mehlhorn, R. J., Serbinova, E., and Kagan, V. E. (1989) *Biochem. Biophys. Res. Commun.* **159,** 229–235
60. Lee, S. M, Koh, H.-J., Huh, T.-L., and Park, J.-W. (1999) *Biochem. Biophys. Res. Commun.* **254,** 647–650
61. Stein, A. M., Stein, J. H., and Kirkman, S. K. (1967) *Biochemistry* **6,** 1370–1379
62. Ravindranath, V., and Reed, D. J. (1990) *Biochem. Biophys. Res. Commun.* **169,** 1075–1079
63. Murakami, K., Kondo, T., Kawase, M., Li, Y., Sato, S., Chen, S. F., and Chan, P. H. (1998) *J. Neurosci.* **18,** 205–213
64. Kehrer, J. P., Paraidathathu, T., and Lund, L. G. (1993) *Proc. West. Pharmacol. Soc.* **36,** 45–52
65. Lund, L. G., Paraidathathu, T., and Kehrer, J. P. (1994) *Toxicology* **93,** 249–262
66. Vogel, R., Wiesinger, H., Hamprecht, B., and Dringen, R. (1999) *Neurosci. Lett.* **275,** 97–100
67. Schreck, R., Rieber, P., and Baeuerle, P. A. (1991) *EMBO J.* **10,** 2247–2258
68. Favreau, L. V., and Pickett, C. B. (1995) *J. Biol. Chem.* **270,** 24468–24474
69. Michikawa, Y., Mazzucchelli, F., Bresolin, N., Scarlato, G., and Attardi, G. (1999) *Science* **286,** 774–779